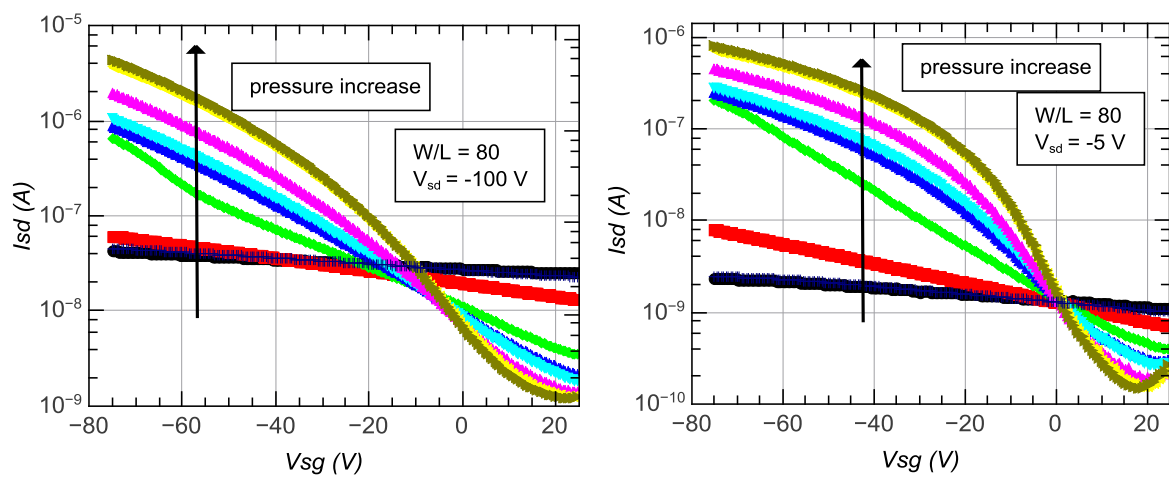
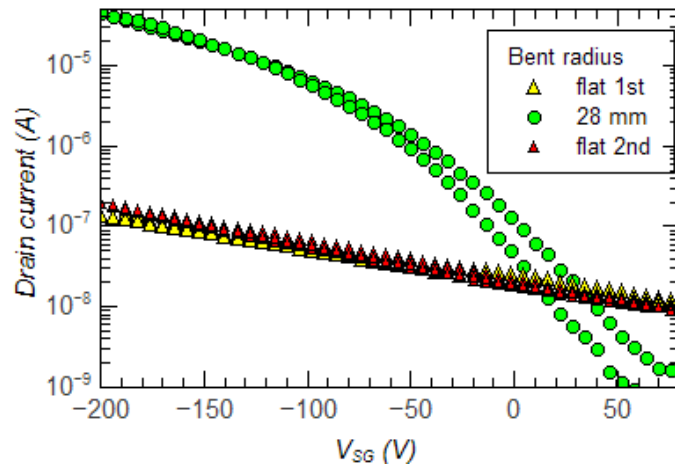


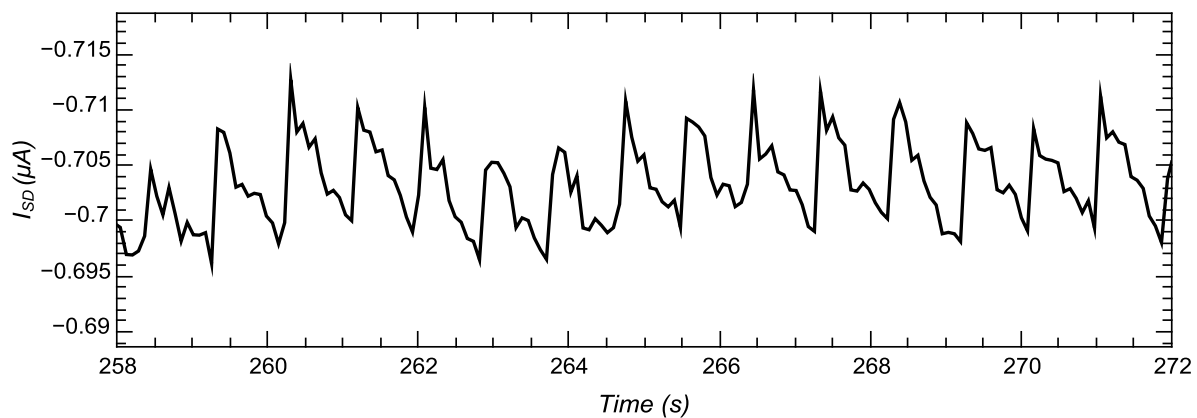
Supplementary Figure S1. Transfer curves at different pressure loads of a pressure sensitive OTFT device. Left: In air right after lamination without further encapsulation and annealing. Right: In a nitrogen atmosphere, after annealing at 80°C for 20 min. Note the low on-off ratios and strong positive threshold voltage shift in air which is indicative of oxygen doping. After short annealing in nitrogen, the doping effect is already strongly reduced which can be seen from the much higher on-off ratios and a negative threshold voltage shift.



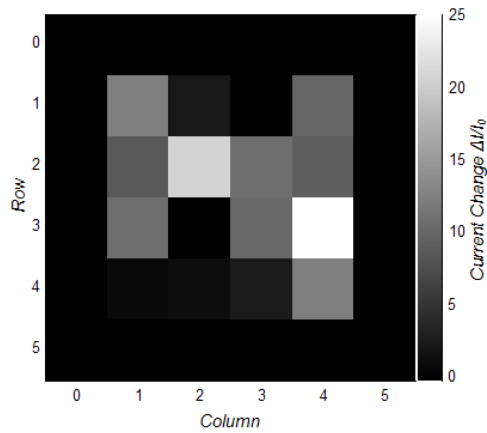
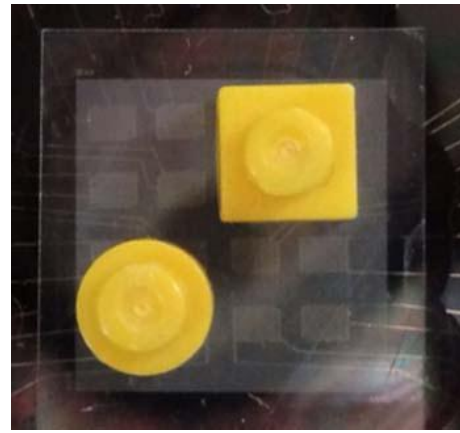
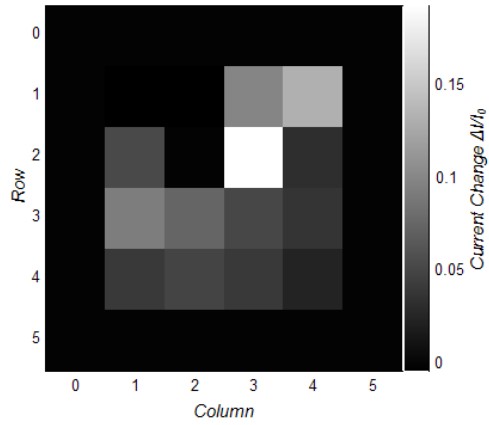
Supplementary Figure S2. Transistor transfer characteristics of the same device as in Figure 3. Measurements are taken varying the applied pressure and the source-drain voltage.



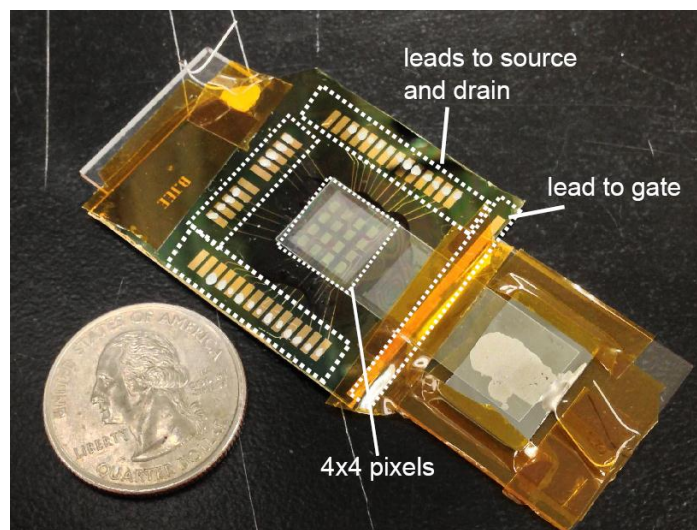
Supplementary Figure S3. Device characteristics recovering after the bending experiment. Device transfer curves before bending (flat 1st), during bending to 28 mm, and after flattening it again (flat 2nd). Source-drain voltage is -200 V.



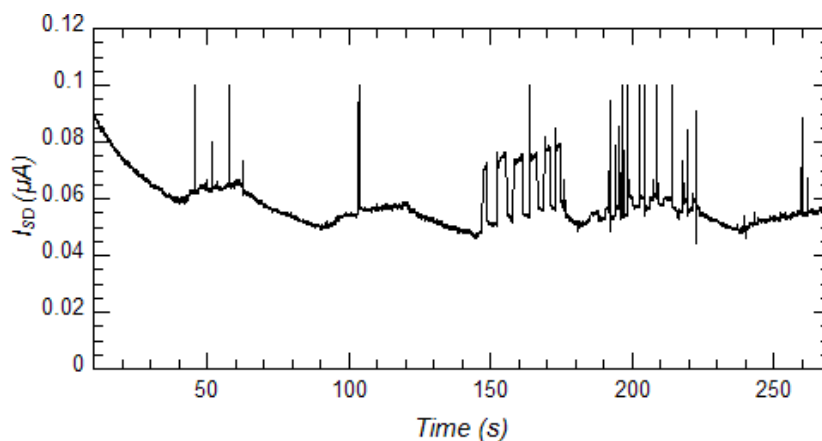
Supplementary Figure S4. Pulse curve measurement at lower driving voltage. The measurement was taken at -36 V source-drain and source-gate voltage, taken with a Keithley 4200 SCS in continuous recording mode.



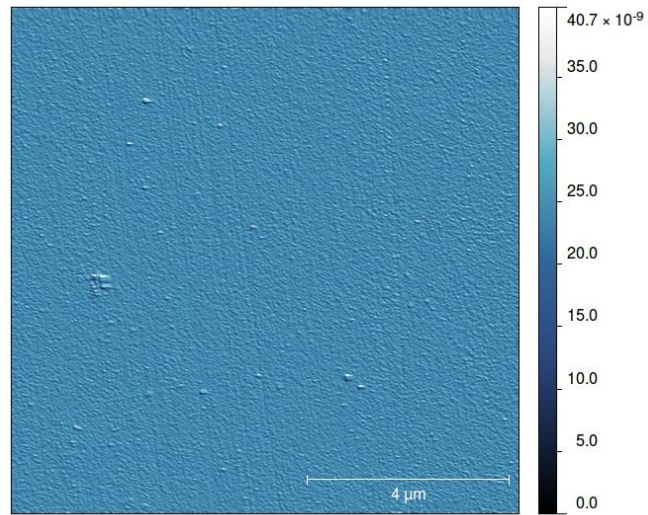
Supplementary Figure S5. Spatial resolution of the array device. Array response (left) to various objects placed as shown in the corresponding picture on the right. Upper: Two objects weighing 50 mg each. Lower: V-shaped object with an additional force of 0.45 N applied. All objects are not perfectly flat. Therefore, the array does not reproduce an exact image of the objects but rather of their contact points.



Supplementary Figure S6. Overview picture of the array. The device is mounted on a glass slide for measurements.



Supplementary Figure S7. Initial current drop during continuous device operation. Time development of the source-drain current while the device was operated under constant source-drain and source-gate voltage of -100V. The spikes correspond to pressure changes upon manually placing various objects onto the sensor. The current decay within the first 100 s is attributed to bias stress effects. Current drift after 100 s is due to changes in illumination.



Supplementary Figure S8. BCB planarisation layer. Atomic force microscope image of the cured BCB layer surface on the polyimide substrate.

Pyramid spacing	1.33 μm	3.79 μm	8.85 μm	13.61 μm	∞ (3 μm air gap only)	3 μm PDMS unstructured
Capacitance measured (nF/cm ²)	0.223	0.212	0.167	0.114		
Capacitance calculated (nF/cm ²)	0.329	0.322	0.307	0.303	0.296	0.692
Average air gap Calculated (μm)	1.28	1.43	2.42	4.83		

Supplementary Table S1. Comparison of measured capacitance and calculated capacitance of the pyramid structures with different spacings. Calculations are for the idealized case of uncompressed pyramid structures between two perfectly parallel electrodes in direct contact with the structures. The deviation between measured and calculated capacitance can be explained by an additional air gap which forms between the structures and the top electrode due to a slightly curved substrate and the electrodes not being perfectly parallel.